International Journal of Marine Engineering Innovation and Research, Vol. 10(4), Dec. 2025. 1082-1090
(pISSN: 2541-5972, eISSN: 2548-1479)

Assessment Seakeeping Performance And Operability Model A Fast Craft Using Axe Bow

Romadhoni Romadhoni[1*], Budhi Santoso[2], IK.A Pria Utama[3]
(Received: 13 October 2025 / Revised: 16 October 2025 /Accepted: 17 October 2025 / Available Online: 1 December 2025)

***Abstract*— Hull shape affects the characteristics of movement and operability ship itself. Operability ship is at sea the amount of time during which the structure is capable of operating in accordance with the criteria established and high correlation to wave in which criteria will be exceeded. In the research will be carried out analysis of three degrees of freedom of movement and pitch roll heave against the ship model-type crew boat planing hull and AXE Bow size 38 meters on a regular wave with future parameter (heading, speed, mass body, radius gyration, damping and etc.) are presented in the form of graphic images Response Amplitude Operator (RAO). Motion prediction in regular waves has been performed by running a mathematical model developed on the basis of a 3-liner potential theory, and further transformed into the motion in irregular waves through the spectral analysis. The calculation is performed with the help of software computing HydroSTAR Ver.7.1 will be compared with Maxsuft software. This latter analysis was conducted for all level of intensities by referring to the wave scatter data for Natuna Sea, and then correlated to the operational criteria. Results of evaluation exhibits that at full load, operational crew boat could be carried out at significant wave heights Hs ranging from 0.245m up to 3.745m, which has a proportion of occurrence as much as 97.02% to model planing hull and as much as 98.72% to model AXE Bow. Crew boat operation would not be safely conducted at wave heights higher than those, in which their occurrence in Natuna Sea is only 2.720%, model hull planing and is only 0.14% model AXE Bow**

Keywords— Fast craft, Axe bow, Planing hull, Seakeeping Performance, Potential theory, HydroSTAR

**Corresponding Author:* romadhoni@polbeng.ac.id

I. INTRODUCTION

The seakeeping performance of a ship is greatly influenced by the size and shape of its hull geometric parameters (main dimensions, beam coefficient, prismatic coefficient, air plane area coefficient, longitudinal location and vertical center of the float, longitudinal position of the center of the water plane) [1].The size of the ship model is very important to consider in comparing alternative designs, which are expected to be capable of operating in the same area. In this study the length of the vessel is considered as an indicator of displacement size[2]. But on the other hand, it is clear that seakeeping operability must be checked at an early stage of fast craft design. For the time being, there are several criteria that apply in the ship model design work process to provide good seakeeping performance. Based on the classification and regulations, non-normative requirements, such as operational and comfort criteria, are related to the physical characteristics of the ship. The operational criteria are explained by the acceleration at a certain point of the hull, the pitching amplitude, and the possibility of slamming and green water shipping phenomena[3]. The AXE bow type is characterized by a stern tilt, starting from the extreme stem point, as well as a narrow V-shaped frame and smooth volume distribution in the bow[4]. This design is intended to reduce the added resistance of the hull by reducing the wet surface and to reduce the dynamic stress generated by the breaking waves[5]. However, in the AXE-bow design, the resulting decrease in bow displacement causes an increase in the pitching and heaving amplitudes, with a resulting increase in the vertical acceleration amplitude[6].

The analysis of this research was carried out on the hydroSTAR and maxsuft advent software, which has shown the advantages of the AX Bow shape compared to the conventional bow[7]. In previous studies, the resistance results were significantly reduced, coupled with seakeeping movements on the hull and acceleration caused by smaller sea waves[8]. Another interesting design is the wave-piercing hull which certainly delivers. Seakeeping is one of the important performances for a Fast Craft[9]. Analysis using a validated numerical model calculation "potential theory". The next step is to analyze the RAO (Response Amplitude Operator), added mass and damping on the variation of boat speed and water depth[10][11]. Further analysis was carried out taking into account the environmental conditions such as significant wave height Hs parameters, such that the amplitude response vessel known for some conditions Hs[11]. [9]

Romadhoni Romadhoni, Politeknik Negeri Bengkalis, Email: romadhoni@polbeng.ac.id

Budhi Santoso, Department Naval architecture, Politeknik Negeri, Bathin Alam Sei. Alam, Bengkalis-Riau, Email: budhisantoso@polbeng.ac.id

IK.A Pria Utama, Department of Naval Architecture, Institut Teknologi Sepuluh Nopember, Surabaya, Indonesia, Email: kutama@na.its.ac.id

II. METHOD

A. Vessel Description & Data Booklet

1) Fast Craft

Fast craft is a marine transportation vehicle used for wearing group or workers who typically work offshore, or in drilling[12]. This vessel operates much like the ship - a passenger deliver in widespread. This form of ship is simply too massive and now not an excessive amount of convey passengers or people, due to the fact this sort of deliver priority to consolation[13].

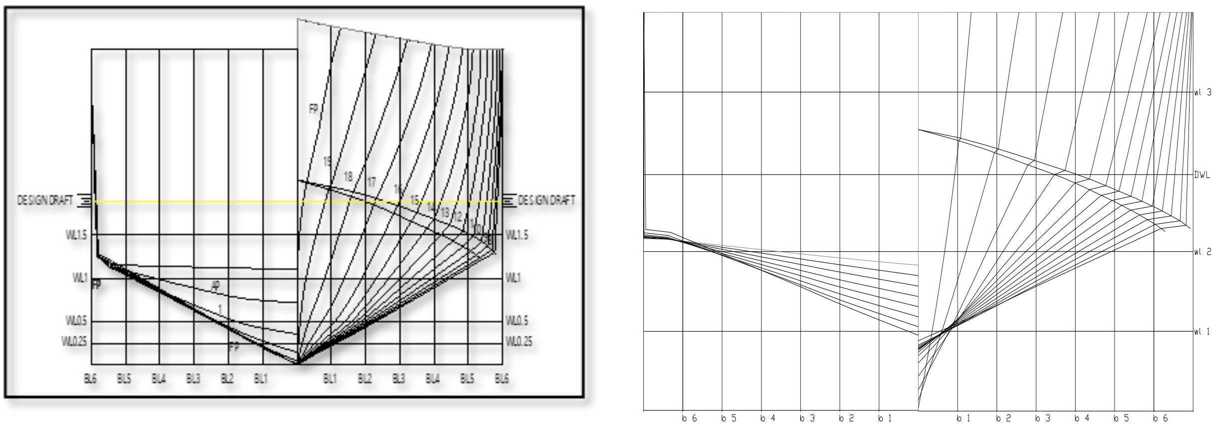

Figure 1. Fast Craft Type Planing and AXE Bow

2) Potential Flow Theory Of Ship in Waves

Assuming the ship moving at an average speed U at certain wave heading to the regular wave amplitudes in the infinite water depth. Ships under oscillating movement disorders wave style[14]. This research will discuss the interaction between waves and ship hydrodynamics in order potential flow theory. With assuming in interaction between waves and ship oscillation achieve periodic state, the potential speed wobble around bodies moving to the coordinate system can be expressed as follows[15]:

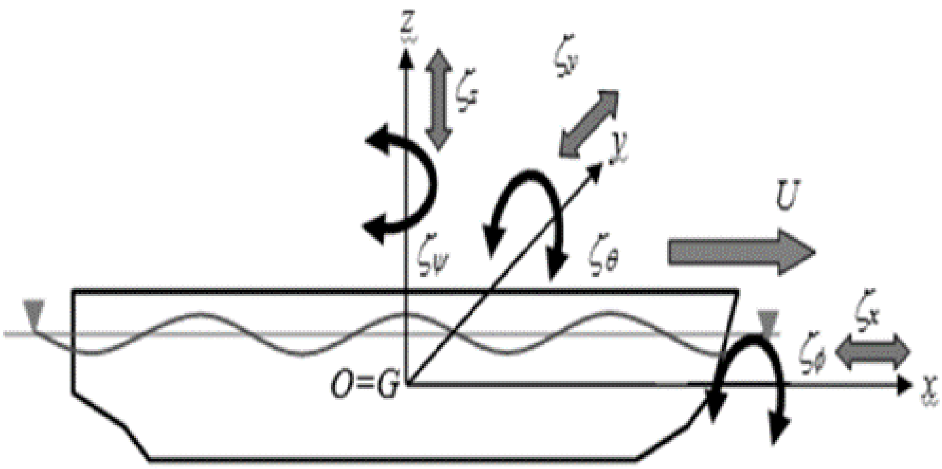

Figure 2. Coordinate Systems Ship Motion

$$\Phi_T(x,y,z,t) = Re\left[\zeta_a + \emptyset_0 + \emptyset_\gamma^0 e^{i\omega t} + \textstyle\sum_{j=n}^{6} i\omega\eta_j \emptyset_j^0\right] \quad (1)$$

In Eq.(l) ζ_ais the Amplitude regular wave, ω is the Encounter frequency ships with progressive wave, Ø_0 is the potential wave with unit amplitude, Ø_γ^0 is the potential wave diffraction due to interference ship wave comes with unit amplitude, ηj (j = 1,2, ... 6) periodic oscillation movement of ships in waves displacement, and Ø_j^0 is the potential wave radiation from periodic oscillation amplitude units ship with the speed in the direction j[16].

The potential value that is not disturbed by the incident wave at the point (X, Y, Z) in the fluid is known from the following equation:

$$\emptyset_I = \frac{-ig\cosh[k(d+Z)]e^{ikt(X\cos\theta+Y\sin\theta)}}{\omega\cosh kd} \quad (2)$$

Where:

d = Depth Water
k = Wave number
θ = Heading wave

The relationship between the wave number 'k' with angular frequency 'ω' as follows[17]:

$$\omega^2 = gk\tanh(kd) \quad (3)$$

Once the potential is known, the first hydrodynamic pressure value can be calculated based on the Bernoulli equation:

$$P = -\rho \frac{\partial \phi}{\partial t} \tag{4}$$

Because the harmonic motion of the Ship, the reaction force equation can be written as follows[16]:

$$F_{ji} = -A_{ji}\ddot{x}_i - B_{ji}\dot{x}_i \tag{5}$$

Where:

$A_{ji} = \frac{\rho}{\omega} \int_S \phi_i^{Im} n_j \, dS$, Added Mass Coefficient

$B_{ji} = \rho \int_S \phi_i^{Re} n_j \, dS$, *Wave Damping Coefficient*

Finally, the ship motion equation could be expressed as:

$$\sum_{n-1}^{6}\left[(M_{jk} + A_{jk})\ddot{\eta_{ka}} + A\dot{\eta}_{jk} + C_{jk}\zeta_{ka}\right] = F_j e^{i\omega t}; \quad j,k = 1,2,\ldots 6 \tag{6}$$

Where:

Mij = Matrix mass moment of inertia and mass of marine construction,
Aij = Matrix coefficients hydrodynamic added mass,
Bij = Matrix hydrodynamic damping coefficients,
Cij = Stiffness matrix coefficients or hydrostatic forces and moments,
Fj = Matrix force excitation (F1, F2, F3) and moments of excitation (F4, F5, F6) in the complex function (declared by it),
F1 = Excitation force which causes movement of surge
F2 = Force excitation causes sway motion
F3 = Force excitation causes heave motion
F4 = Moment of excitation that causes movement of the roll
F5 = Moment excitation causes the pitch movement
F6 = Moment excitation causes a yaw movement
Zk = Elevation movement mode to k,
$\ddot{\eta_{ja}}$ = Elevation velocity of the mode to k,
$\dot{\eta}_{ij}$ = Elevation motion acceleration mode to k.

If assumes that the ship has a symmetrical shape of the upright O-xz plane and center of gravity the coordinates (0.0, ZG) the general mass matrix is[18]:

$$\mathbf{M}= \begin{bmatrix} M & 0 & 0 & 0 & M.Z_{GC} & -M.Y_{GC} \\ 0 & M & 0 & -M.Z_{GC} & 0 & M.X_{GC} \\ 0 & 0 & M & M.Z_{GC} & -M.X_{GC} & 0 \\ 0 & -M.Z_{GC} & M.Y_{GC} & I_{44} & I_{45} & I_{46} \\ M.Z_{GC} & 0 & -M.X_{GC} & I_{54} & I_{55} & I_{56} \\ -M.Y_{GC} & M.X_{GC} & 0 & I_{64} & I_{65} & I_{66} \end{bmatrix}$$

Where:

M = is the mass of the body
$X_{GC} = X_G - X_{cal};$
$Y_{GC} = Y_G - Y_{cal};$
$Z_{GC} = Z_G - Z_{cal};$

Where:

+ X_{GC}, Y_{GC}, Z_{GC} being the position of the centre gravity in the mesh
+ $X_{cal}, Y_{cal}, Z_{cal}$ being the position of the calculation point.

$I_{44} = \int_M [(y - Y_{Cal})^2] + [(z - Z_{Cal})^2]dm = M\,(R_{44}^2 + Z_{GC}^2 + Y_{GC}^2)$

$I_{55} = \int_M [(z - Z_{Cal})^2] + [(x - X_{Cal})^2]dm = M\,(R_{55}^2 + Z_{GC}^2 + X_{GC}^2)$

$I_{66} = \int_M [(x - X_{Cal})^2] + [(y - Y_{Cal})^2]dm = M\,(R_{66}^2 + X_{GC}^2 + Y_{GC}^2)$

$I_{45} = I_{54} = -\int_M [(x - X_{Cal})\ ] + [(y - Y_{Cal})\ ]dm = M\,(R_{54}^2 + X_{GC} + Y_{GC})$

$I_{46} = I_{64} = -\int_M [(x - X_{Cal})\ ] + [(y - Y_{Cal})\ ]dm = M\,(R_{64}^2 + X_{GC} + Y_{GC})$

$I_{56} = I_{65} = -\int_M [(x - X_{Cal})\ ] + [(z - Z_{Cal})\ ]dm = M\,(R_{56}^2 + X_{GC} + Z_{GC})$

$I_{56} = I_{65} = -\int_M [(y - Y_{Cal})\ ] + [(z - Z_{Cal})\ ]dm = M\,(R_{54}^2 + Y_{GC} + Z_{GC})$

With:

M : The mass the body
X_{GC}, Y_{GC}, Z_{GC} : The center of Gravity
$R_{44}, R_{55}, R_{66}, R_{45}, R_{46}, R_{56}$: The gyration radius

Where:

$R_{ii} = \sqrt{\frac{I_{ii}}{M}}$ with respect to be COG

$R_{ij} = \text{sign}\,(I_{ij}) = \sqrt{\frac{|I_{ij}|}{M}}$ with respect to be COG

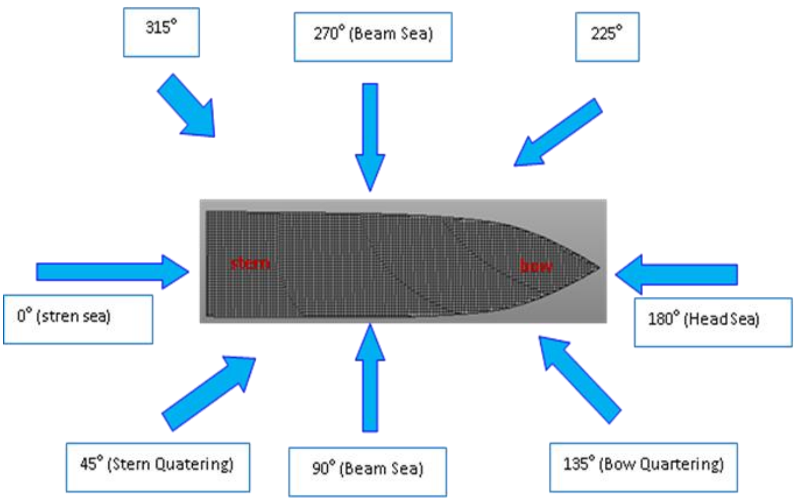

Figure 3. Orientations angle of incident wave

3) The Input Parameters Of Model Tests And Numerical Computatio

To determine the hydrodynamic characteristics of a ship, it will be presented in the form of the characteristics of movement - a movement that is commonly experienced by the ship at the time of sailing[19]. Characteristics of these movements will be presented in the form of movement heave, roll and pitch with speed variation 0 knots, 12 knots, and 25 knots on a heading angle 0, 45, 90, 135, and 180[20].

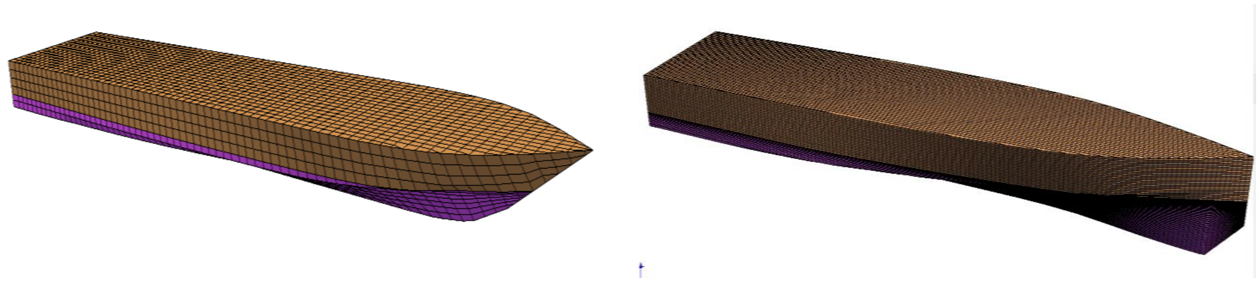

(a) HPC : Hull Planing Chine (b) HPCAB : Hull Planing Chine AXE Bow

Figure 4. Model Crew boat ship by HydroStar Software

TABLE 1.
DESIGN PARAMETERS CREW BOAT SHIP

Parameter	Sym	Unit	HPC	HPCAB
Overall Length	LOA	m	38	38
Length Water line	LWL	m	35.5	38
Breadth Molded	Bmld	m	7.6	7.6
Height Molded	Hmld	m	3.65	3.65
Draft/Drought	T	m	1.89	1.89
Displacement	Δ	Ton	240.5	240.59
Coefficient Prismatic	Cp	m	0.795	0.718
Coefficient Block	Cb	M^2	0.46	0.32
Coefficient Midsip	Cm	m	0.624	0.644
Water Surface Area	WSA	m	284.05	293.56

In table 2. from the modeling can be continued for running. Based on the results obtained from HidroStar and Maxsuft difference of each model is less than 1%, the difference is not too large so that the ship models are made in the program software maxsuft and hydroSTAR is correct so it can the calculation and next analysis[21].

4) Righting-Arm (GZ) Curve Generation Centre Gravity and Radius Gyration

There are important parameters that need to be known to calculate the motion of a ship[22]. As it is known that the vessel or other object moving with center gravity, so for this case was the focus needs to be known. Calculate the radius gyration[23].

$$\text{For Ship } K_{xx} = 0.30.B \text{ to } 0.4.B \quad K_{yy} = 0.22.L \text{ to } 0.28.L \quad K_{zz} = 0.22.L \text{ to } 0.28.L \tag{8}$$

Where L is the length of ship and B is the Breadth of ship, aaccording to the radius of gyration Bureau Veritas roll:

$$K_{xx} = 0.289.\ B\ .\left(1\left(\frac{2.KG}{B}\right)^2\right) \tag{9}$$

5) Roll Dumping Coefficient

The dimensional damping coefficient Bhattacharyya is[24]

$$B_{44} = \beta_{44}\ 2\sqrt{C_{44}(I_{44}+A_{44})} \tag{10}$$

β_{44} $= \frac{v}{\omega_0}$ (non dimensional input)

I_4 = mass inertia of vessel in roll = $k_{xx}^2 \nabla\rho$

A_{44} = added inertia coefficient for roll = $0.3I_4$

C_{44} = hydrostatic restoring coefficient = $GM_T\nabla\rho g$

HydroStar then linearize the quadrating damping in absolute value for ship. Molin suggest[25]:

$$+B_Q = \frac{1}{2}\rho C_D B^4 L \tag{11}$$

Where:

ρ = is the fluid density

B = is the ship width

L = is the ship Length

C_D =is a coefficient with scales around 0.1 - 0.2

6) Sea States and Spectrum

Water conditions in this study refers to the condition (Sea State Code) which has been established by WMO (World Meteorological Organization) with a review of the four (4) variations in sea conditions with different parameters include the third highest wave height (significant wave height), period waves (wave period), and wind speed (Sustained wind Speed)[26]. Variation sea conditions are small waves (slight), medium waves (moderate) large waves (rough) and very waves (very rough). Sea state code used is 3, 4, 5 and 6, are shown in Table 3.

Next by using the formula JONSWAP, wave spectrum can be determined by Hs as input, even though other approaches are also possible such as Bretschneider 1959 and 1969, Pierson Moskowitz, 1964. The following JONSWAP wave spectrum is used in model test and numerical simulation for the seakeeping evaluation of the Crew Boat Ship[27]:

$$S_\omega(\omega) = A\,x\,\frac{5}{16}H_s^2\omega_p^4\omega^{-5}exp\left[-\frac{5}{4}\left(\frac{\omega}{\omega p}\right)^{-4}\right]_\gamma\left[exp\left(\frac{-(\omega-\omega p)}{2\sigma^2\omega_p^2}\right)\right] \quad (12)$$

Where:

$A = \frac{1}{5.(0.065.\gamma^{0.803}+0.0135}$

σ = 0.07 for $\omega < \omega p$ and $\sigma = 0.09$ for $\omega > \omega p$

$\omega p = 2\pi(g/Uw)(X_0)^{-0.33}$

$X_0 = gX/U_w^2$

U_w = Wind speed

X = Lengh fetch

Responds Spectrum

$$S_R = [RAO(\omega)]^2 S(\omega) \quad (13)$$

7) Response Parameters

In this paper, response are used as bellow:

1. RAO Heave η_{3a}/ζ_a
2. RAO Roll $\eta_{4a}/k\zeta_a$
3. RAO Pitch $\eta_{5a}/k\zeta_a$
4. Respond Spectrum $[RAO(\omega)]^2S(\omega)$

The variable in the above parameter are defied below: ζa regular wave amplitude, k wave number, $\eta 3a$, $\eta 4a$, $\eta 5a$ heave, roll and pitch motion amplitude, ρ water density, g gravity acceleration, B bread, and L ship length between perpendicular.

III. RESULTS AND DISCUSSION

A. The Comparison Of Ship Motion In Regular Head Waves

Figs. 5 and 6. In regular head waves, the numerical responses including response amplitude operator (RAO) of heave and pitch those from the model Hull planing and model AXE Bow Figs.5 test results. Present the comparison at the forward speed of 0, 12 and 25 knot. In these figures, the scattered points represent the results from software maxsuft. While the solid curve represents the results from the 3-D linear hydrodynamic analysis using Hydroster software.

B. Compute Hydrostatic Parameters The comparison of ship motion in regular beam waves at zero forward speed

Figs. present the RAO response of roll, and heave motion at bow and stem positions in beam regular wave at zero forward speed. In the numerical prediction of roll motion using Hydrostar software, the roll damping coefficient in formula (10 and 11) obtained from free decay curve of rol1 motion is used as the rol1 damping. It is seen from the comparison that the numerical results show close agreement with the model test data in the beam regular seas at zero forward speed.

C. Analytics Motion Model

Motion analysis is performed to determine performance ship movement when on the outside due to the force of the waves, the analysis using the method of approach panel method. Analysis was performed on the model Planing Hull Chine (HPC) with Hull Planing Chine AXE Bow (HPCAB).

Having obtained the motion response for the desired conditions in table 4 crates then performed comparing each motion on chine planing hull models (HPC) and model planing hull Chine AXE Bow (HPCAB) comparison is done at an angle of 0, 45, 90, 135 and 180 show in fig 8 following:

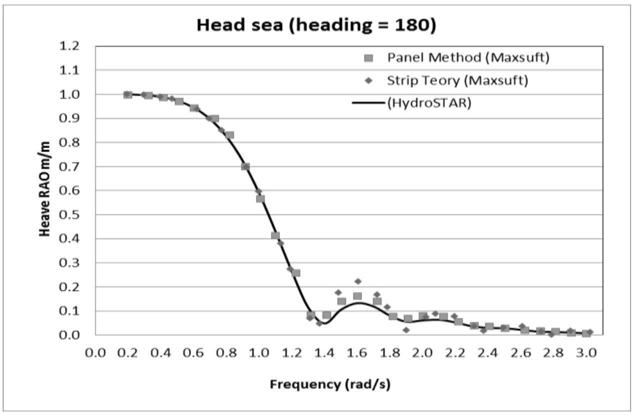

(a)

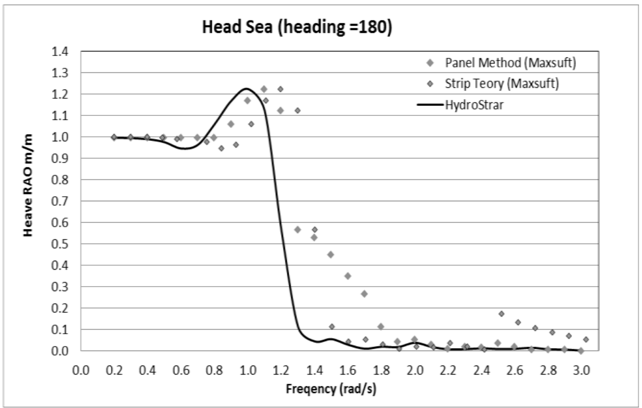

(b)

Figure 5. (a) Heave RAO in head wave at Vs 0 m/s, 6.1728 m/s and Heave RAO in head wave at 12.86 m/s

D. Selection Model Based Response

The quality movement can't be judged only by the RAO or other parameters spontaneously, there needs to be a model response analysis. It really depends on the position where the ship must sail, because it is related to environmental conditions such as wave height in years. In other words, both the poor quality of movement is dependent environmental conditions.

Figure 9 shows the plot between significant wave rises to significant amplitude roll motions. Seen that the significant wave height in the range 1 to 6 m, the model HPCAB produce roll angle is the smallest compared to model HPC. As for the wave height above 1 m HPCAB models have the lowest roll angle. So if concluded, HPC models are most appropriate model when operated in calm sea area with Hs <3 m, whereas for relatively higher wave Hs> 3 m, the model is more feasible for AXE Bow selected.

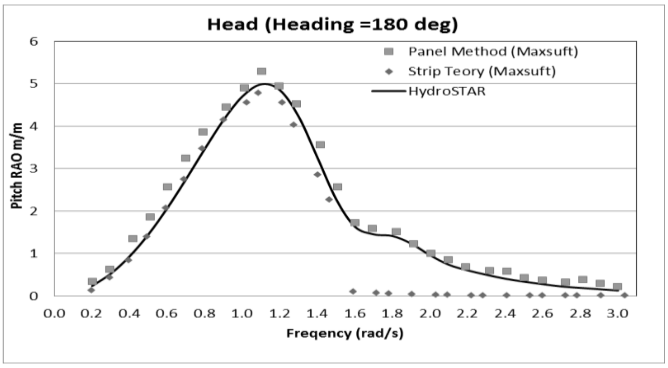

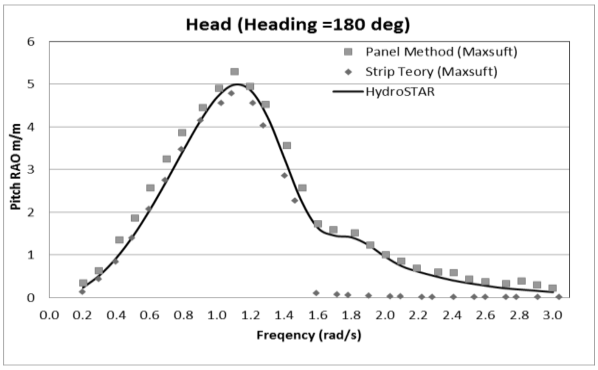

(c) (d)

Figure 6. (c) Pith RAO in head wave at Vs 0 m/s, 6.1728 m/s and (d) Pith RAO in head wave at 12.86 m/s

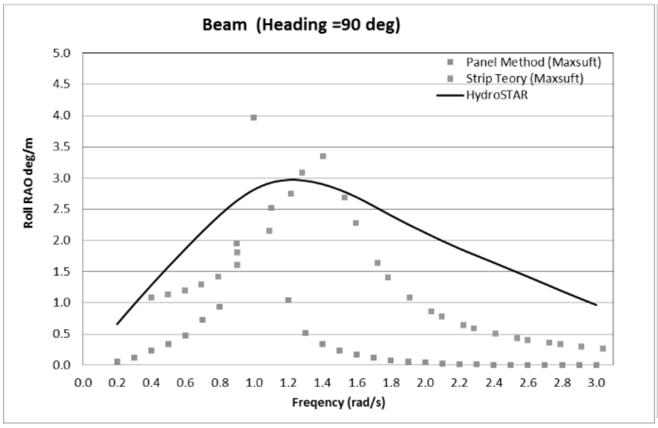

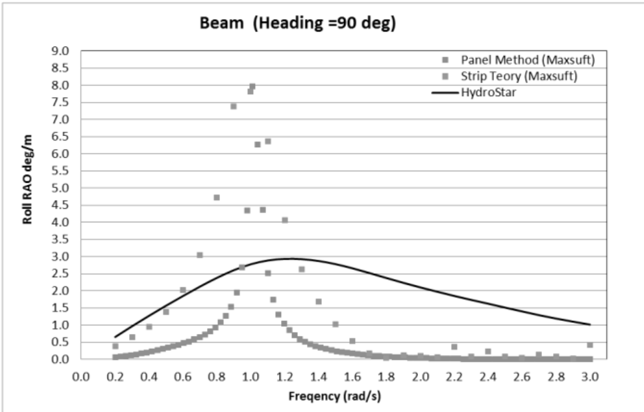

(e) (f)

Figure 7. (e) Heave RAO in head wave at Vs (f) 0 knot model HPC

Fig 10. shows the ship rolling motion, model HPC and HPCAB, which occur with regular wave simulation for 5 minutes on the condition Hs = 2 m, 4 m, and 6 m. It is seen that the peak of the ship heeling angle, roll significant amplitude.

Figure 10n shows the results of calculating the roll response to the HPC and HPCAB models in the Hs 1 irregular wave condition with a speed of 12.68 m/s with a time of 300 seconds which produces a large angle that is relevant to the value in the regular wave for different Hs values. Hull Planing Chine AX Bow has a higher response value than hull planing chine or conventional hull models, the largest response value occurs in 12

seconds with a response value of 2.24 deg for the HPCAB model while 2.09 deg for the HPC bow model. Irregular waves are the sum of similar regular waves by varying their wavelengths, so that random wave heights are obtained, but remain in a range that is not far from the regular wave height.

TABLE 2.
SEAKEEPING MODEL HULL PLANING CHINE AXE BOW (HPCAB)

Information	Difference and seakeeping Value Ratio Comparison				
Angle	0	45	90	135	180
Heave motion (m)	0.001	0	-0.027	0.006	0.01
	2.70%	0.00%	-2.70%	0.60%	1.00%
Roll motion (deg)	0	-0.05	0.09	-0.14	0
	0.00%	-12.50%	16.36%	-34.15%	0.00%
Pitch motion (deg)	-0.01	0.02	-0.08	0.01	0.27
	-2.56%	3.23%	-27.59%	1.32%	60.00%

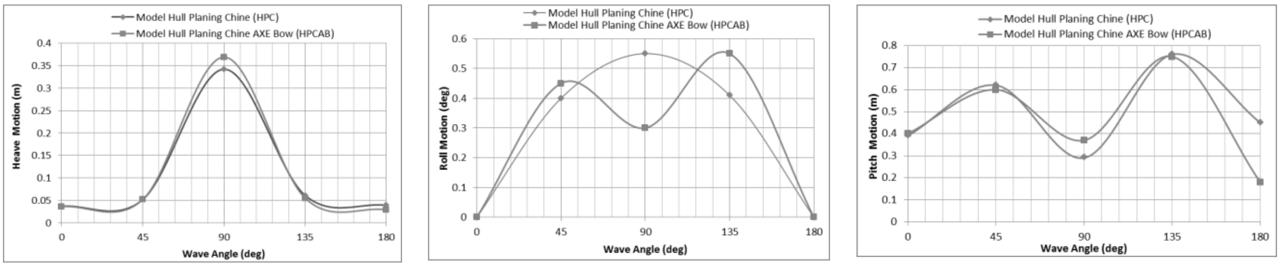

Figure 8. Comparison chart heave motion at variation speed

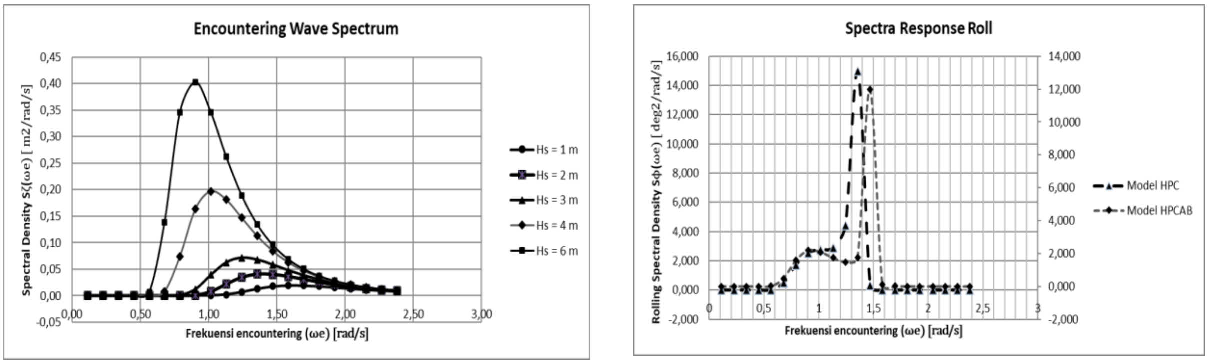

Figure 9. (k) Encountering Wave Spectrum JONSWAP; (l) Spectra Rresponse Roll speed = 12.86 m/s.

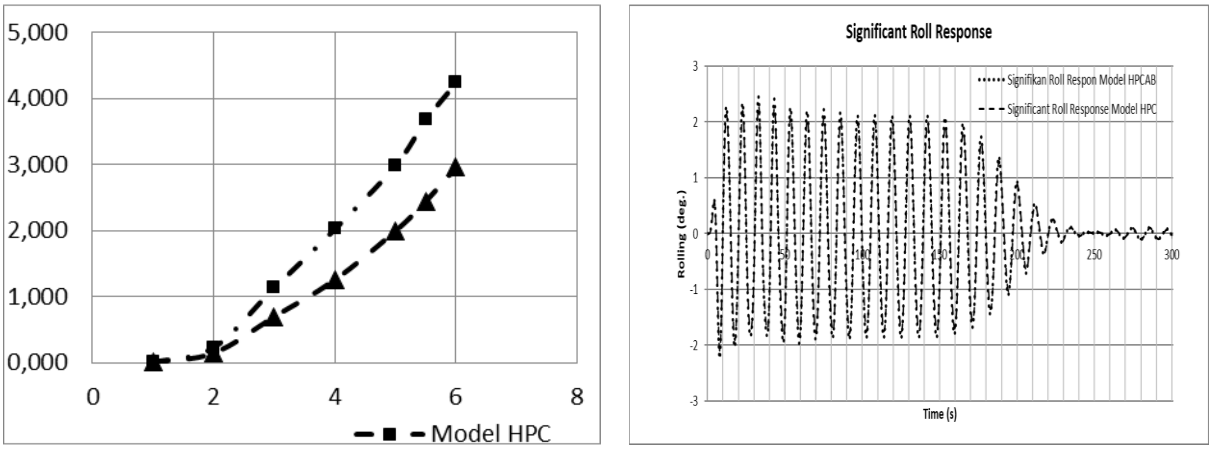

Figure 10. (m) Significant Roll Amplitude Model HPC and HPCAB speed = 12.86 m/s.; (n) Roll Respon Model HPC and HPCAB speed = 12.86 m/s Angle 90o

IV. CONCLUSION

The range of 1 - 6 m significant wave height HPCAB models produce the smallest roll angle compared with HPC models. As for the wave height above 1 m models ROF 8 has the lowest roll angle. In research for the center of gravity height and roll radius of inertia must be managed to ensure good seakeeping performance. Via investigation, concluded that performances better seakeeping of the designers can be achieved by optimization of the design parameters in the early stages of design.

REFERENCES

[1] Y. Liu, N. Ren, and J. Ou, 'Hydrodynamic analysis of a hybrid modular floating structure system under different wave directions', *Applied Ocean Research*, vol. 126, p. 103264, Sep. 2022, doi: 10.1016/j.apor.2022.103264.

[2] M. Yasir, S. Liu, X. Mingming, J. Wan, S. Pirasteh, and K. B. Dang, 'ShipGeoNet: SAR Image-Based Geometric Feature Extraction of Ships Using Convolutional Neural Networks', *IEEE Transactions on Geoscience and Remote Sensing*, vol. 62, pp. 1–13, 2024, doi: 10.1109/TGRS.2024.3352150.

[3] D. Liu, F. Li, and X. Liang, 'Numerical study on green water and slamming loads of ship advancing in freaking wave', *Ocean Engineering*, vol. 261, p. 111768, Oct. 2022, doi: 10.1016/j.oceaneng.2022.111768.

[4] F. Gaspersz, A. Tupamahu, R. B. Luhulima, and S. Tubalawony, 'Study of Purse Seine Fishing Ship Trimaran Seakeeping with Axe-Bow and Without Axe-Bow Model Using Computational Fluids Dynamics', *Kapal: Jurnal Ilmu Pengetahuan dan Teknologi Kelautan*, vol. 20, no. 1, Feb. 2023, doi: 10.14710/kapal.v20i1.47092.

[5] M. Iqbal, M. Terziev, T. Tezdogan, and A. Incecik, 'Hull form optimisation to minimise the total resistance and dynamic responses of small fishing vessels', *Ocean Engineering*, vol. 321, p. 120357, Mar. 2025, doi: 10.1016/j.oceaneng.2025.120357.

[6] M. Sulman, S. Mancini, and R. N. Bilandi, 'Numerical Investigation of Single and Double Steps in Planing Hulls', *J Mar Sci Eng*, vol. 12, no. 4, p. 614, Apr. 2024, doi: 10.3390/jmse12040614.

[7] M. R. Utina, I. M. Ariana, and D. Purnamasari, 'Comparative Analysis on the Effect of Bow Shapes on the Ship Resistance using CFD Simulation and Model Test', *CFD Letters*, vol. 17, no. 3, pp. 36–51, Oct. 2024, doi: 10.37934/cfdl.17.3.3651.

[8] S. Suardi, T. Hidayat, M. B. Firmansyah, and A. Y. Kyaw, 'Impact of Axe Bow Hull Shape on Patrol Ship Resistance, Freeboard, and Trim', *Maritime Park Journal of Maritime Technology and Society*, pp. 16–21, Feb. 2023, doi: 10.62012/mp.v2i1.25478.

[9] I. K. A. P. Utama *et al.*, 'Seakeeping Performance of Warship Catamaran under Varied Hull Separation and Wave Heading Conditions', *Pomorstvo*, vol. 38, no. 2, pp. 275–296, Dec. 2024, doi: 10.31217/p.38.2.9.

[10] S. Nam, J.-C. Park, J.-B. Park, and H.-K. Yoon, 'CFD-Modified Potential Simulation on Seakeeping Performance of a Barge', *Water (Basel)*, vol. 14, no. 20, p. 3271, Oct. 2022, doi: 10.3390/w14203271.

[11] E.-H. Min and M. Kim, 'Fully nonlinear wave interaction with 2D floating body including nonlinear sloshing tank', *Ocean Engineering*, vol. 307, p. 118063, Sep. 2024, doi: 10.1016/j.oceaneng.2024.118063.

[12] S. V. Sagin *et al.*, 'Ensuring the safety of maritime transportation of drilling fluids by platform supply-class vessel', *Applied Ocean Research*, vol. 140, p. 103745, Nov. 2023, doi: 10.1016/j.apor.2023.103745.

[13] A. Lepore, L. Mocerino, B. Palumbo, E. Rizzuto, E. Rossi, and L. Vitiello, 'A supervised statistical learning approach to the preliminary design of cruise ship Gross Tonnage', *Applied Ocean Research*, vol. 143, p. 103837, Feb. 2024, doi: 10.1016/j.apor.2023.103837.

[14] Z. Chen, J. Jiao, X. Chang, and B. Ma, 'Numerical and experimental study of asymmetrical wave loads and hydroelastic responses of ship in oblique regular waves', *Applied Ocean Research*, vol. 153, p. 104254, Dec. 2024, doi: 10.1016/j.apor.2024.104254.

[15] R. Kumar and R. K. Mitra, 'Stability of Periodic Orbits and Bifurcation Analysis of Ship Roll Oscillations in Regular Sea Waves', *International Journal of Bifurcation and Chaos*, vol. 33, no. 05, Apr. 2023, doi: 10.1142/S021812742350058X.

[16] X. Zhang, X. Song, and R. F. Beck, 'Numerical investigations on seakeeping and added resistance in head waves based on nonlinear potential flow methods', *Ocean Engineering*, vol. 276, p. 114043, May 2023, doi: 10.1016/j.oceaneng.2023.114043.

[17] K. Shi, R. Zhu, M. Zheng, and C. Li, 'Simulation of ship motion response in head seas using a fully nonlinear potential flow method', *Ocean Engineering*, vol. 309, p. 118309, Oct. 2024, doi: 10.1016/j.oceaneng.2024.118309.

[18] Y. Zhang, Y. Pu, and Z. Hu, 'A mathematical and numerical model for variable cross-section hull girder with time-varying mass systems applied in marine vessels', *Marine Structures*, vol. 101, p. 103726, Apr. 2025, doi: 10.1016/j.marstruc.2024.103726.

[19] S. Ding *et al.*, 'Research on inland ship hydrodynamic modeling and parameter identification based on CFD', *Ocean Engineering*, vol. 318, p. 120064, Feb. 2025, doi: 10.1016/j.oceaneng.2024.120064.

[20] M. B. S. Putrananda, A. Bahatmaka, W. Aryadi, B. A. Puteri, and C. I. Hutagalung, 'Numerical Analysis of Six Degrees of Freedom Motion Response of Trimaran Semi-Submersible Ship', *Mekanika: Majalah Ilmiah Mekanika*, vol. 24, no. 1, p. 61, Mar. 2025, doi: 10.20961/mekanika.v24i1.99057.

[21] M. Bhatia, N. Das, P. Dutta, and H. Chattopadhyay, 'Numerical analysis on the seakeeping performances of a full-scale container ship hull using strip theory', *Physics of Fluids*, vol. 35, no. 11, Nov. 2023, doi: 10.1063/5.0172626.

[22] M. Iqbal, M. Terziev, T. Tezdogan, and A. Incecik, 'Hull form optimisation to minimise the total resistance and dynamic responses of small fishing vessels', *Ocean Engineering*, vol. 321, p. 120357, Mar. 2025, doi: 10.1016/j.oceaneng.2025.120357.

[23] A. Trimulyono *et al.*, 'Numerical Investigations of Deckhouse Height to the Self-Righting Moment of the Patrol Boat', *Designs (Basel)*, vol. 8, no. 5, p. 86, Aug. 2024, doi: 10.3390/designs8050086.

[24] E. Hwang and K.-K. Yang, 'Numerical Analysis of Roll Hydrodynamic Coefficients of 2D Triangular Cylinder Using OpenFOAM', *J Mar Sci Eng*, vol. 13, no. 3, p. 391, Feb. 2025, doi: 10.3390/jmse13030391.

[25] A. Big-Alabo and D. Koroye, 'Nonlinear vibration analysis of the large-amplitude asymmetric response of ship roll motion', *Ocean Engineering*, vol. 243, p. 110088, Jan. 2022, doi: 10.1016/j.oceaneng.2021.110088.

[26] H. Li *et al.*, 'A Novel Sea State Classification Scheme of the Global CFOSAT Wind and Wave Observations', *J Geophys Res Oceans*, vol. 129, no. 11, Nov. 2024, doi: 10.1029/2023JC020686.

[27] T. Hanaki, N. Sogihara, and M. Tsujimoto, 'Reproducibility evaluation of detailed directional spectrum based on mean spreading angle for ship performance estimation in actual seas', *J Mar Sci Technol*, vol. 29, no. 3, pp. 711–724, Sep. 2024, doi: 10.1007/s00773-024-01022-2.